

The SPV NO₂ Gas Sensor Fabricated by Mesoporous Tin Oxide Film

Brian Yuliarto,^{†,††} Haoshen Zhou,^{*†} Takeo Yamada,[†] Itaru Honma,[†] and Keisuke Asai^{††}

[†]Energy Electronic Institute, National Institute of Advanced Industrial Science and Technology (AIST),
1-1-1 Umezono, Tsukuba 305-8568

^{††}Department of Quantum Engineering and System Science, Graduate School of Engineering,
The University of Tokyo, 7-3-1 Hongo, Bunkyo-ku, Tokyo 113-8565

(Received February 26, 2003; CL-030165)

A highly sensitive NO₂ gas sensor was successfully fabricated by mesoporous tin oxide film based on surface photo voltage (SPV). The sensor measured the changes of the average value of AC photocurrent and has detection level as low as 1 ppm of NO₂ gas.

NO₂ is one of the most dangerous gas related to the health and environmental damage.¹ This factor has forced researchers to develop trustworthy and reliable NO₂ gas sensor.^{2,3} Among semiconductor oxide materials, it is well-known that tin oxide is the most widely used to detect reducing gases as well as oxidizing gases. The benefits of using SnO_x as a gas sensor include high sensitivity at relatively low temperatures, low cost, fast response, and high mechanical strength.^{4,5} One of the modifications that strongly relates to improving sensor performance is enlarging the surface area.⁶⁻⁸ Recently, mesoporous materials have attracted much attention because of their high surface area and uniform pore size. The mesoporous tin oxide powder has been investigated for CO and H₂ sensor.⁷ However, there is no reported research about the mesoporous thin films based on tin oxide for gas sensor application. This paper is the first study to our knowledge of the preparation and the application of mesoporous tin oxide films as NO₂ gas sensors. The SPV system is used to characterize the sensor, because it is well-known that this technique is a powerful method to detect the gas pollutants.⁹⁻¹³

Mesoporous tin oxide films used in this study were synthesized by spin coating method using P-123 block copolymer as templates, and a simple chemical solution (SnCl₄) as an inorganic precursor.¹⁴ The typical molar composition of each constituent was SnCl₄/ EtOH/ P-123 block copolymer = 1/21.739/ 0.008. The films were then heated at 40 °C and 50% of relative humidity for 48 h, and calcined to remove the organic template from the materials at 300 °C for 5 h.

The small angle X-ray diffraction profiles are shown in Figure 1. The appearance of sharp and strong peak at low angles (around $2\theta = 0.9^\circ - 1^\circ$) of the synthesized films (Figure 1A) indicates that the mesostructure of tin oxide was formed in the film. The mesostructure reveals two peaks with a d spacing of 9.4 nm and 4.8 nm, which can be indexed as the (100) and (200). Therefore, the XRD pattern of the calcined sample still reveals a peak as shown in Figure 1B. The peak position shifts slightly into the high angle indicating that the d spacing slightly decreased owing to the calcination process. This XRD pattern gives evidence that a mesoporous tin oxide film was successfully prepared using block copolymer as template.

The nitrogen adsorption desorption isotherm is of type IV as illustrated in Figure 2 which is typical for mesoporous mate-

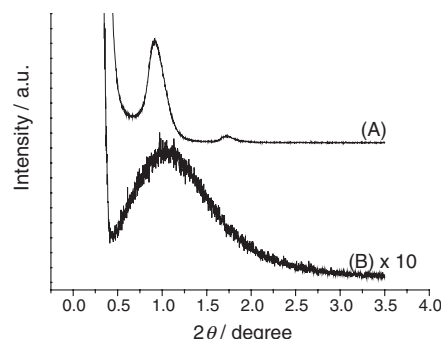


Figure 1. The small angle XRD patterns of mesoporous tin oxide films as synthesized (a), and as calcined at 300 °C for 5 h (b).

rials, with an inflection around a relative pressure P/P_0 of 0.4, corresponding to capillary condensation within uniform mesopores.¹⁵ The Brunauer–Emmet–Teller (BET) specific surface area is 87.3 m²/g. The pore size distribution calculated by Dollimore–Heal (DH) plot is shown in the inset graph of Figure 2. From this plot, the pore radius of the film is 1.8 nm.

The gas sensor devices were prepared as metal insulator semiconductor (MIS) capacitors. The sensor layer of mesoporous tin oxide was fabricated on a Si₃N₄ layer by spin coating, so that the film structure was Au/ SnO₂ (meso) / Si₃N₄/ SiO₂/ Si/ Al, as shown in Figure 3. The AC photocurrent (I_{ph}) flowing through the MIS region was measured as a function of bias voltage (V_{bias}) applied between the Au and Al electrodes.^{9,10,13} The

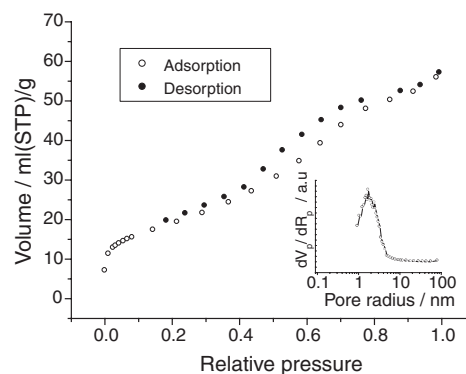


Figure 2. Nitrogen adsorption desorption isotherm (77 K) of mesoporous tin oxide film, and its corresponding pore size distribution (inset). The sample was obtained from scraped mesoporous SnO₂ films.

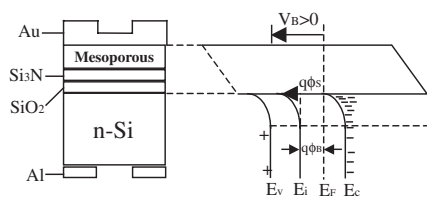


Figure 3. The cross section of SPV sample and its band diagram, where: ϕ_s , ϕ_B , V_B , E_F , E_i , E_c , and E_v correspond to surface potential, potential difference between Fermi level and intrinsic Fermi level, bias voltage, Fermi level, intrinsic Fermi level, conduction band level, and valence band level, respectively.

sensing principle is based on the detection of semiconductor surface charge and surface potential change due to physical absorption and chemical reaction, which are produced by the interaction between gas sensor film and NO_2 gas. Subsequently, the sensing performance of NO_2 gas can be derived from the shift of the $I_{\text{ph}}-V_{\text{bias}}$ diagram characterization. The sensor sensitivity, S , is defined as:

$$S = \frac{(I_{\text{NO}_2} - I_{\text{N}_2})}{I_{\text{N}_2}} \times 100\% \quad (1)$$

Where I_{NO_2} and I_{N_2} are the average photocurrents in NO_2 and N_2 , respectively.

There are three cases occurring at the semiconductor surface when the bias voltage is applied in the MIS structure.^{9,10,13}

Those cases depend on the relation between surface potential (ϕ_s) and the potential difference between the Fermi level and the intrinsic Fermi level (ϕ_B) as shown in Figure 3. The three cases are accumulation ($\phi_s > 0$), depletion ($\phi_B < \phi_s < 0$), and inversion ($\phi_s < \phi_B$). The sensitivity (S) of exposed NO_2 gas at 1 ppm and 800 sccm was estimated by the induced photocurrent through the MIS structure.

The typical plots of photocurrents (I_{ph}) as a function of applied bias voltage (V_{bias}) of the tin oxide mesoporous SPV device are shown in Figure 4, which were measured in N_2 and in the presence of 1 ppm NO_2 at room temperature. From the

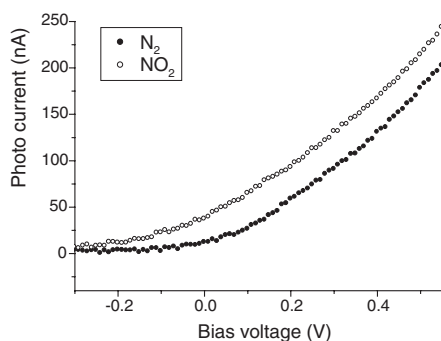


Figure 4. $I_{\text{ph}}-V_{\text{bias}}$ typical curve as exposure of N_2 and NO_2 .

Figure 4, it is obvious that the $I_{\text{ph}}-V_{\text{bias}}$ curves are shifted because of exposure of 1 ppm NO_2 gas. The shift of the photocapacitive current curve along the voltage axis indicated that the positive surface potential was changed owing to the reaction between the NO_2 gas and the mesoporous layer. Moreover, the $I_{\text{ph}}-V_{\text{bias}}$ diagram shift gives significant information relating to the sensor's sensitivity. The sensitivity of the mesoporous tin oxide SPV sensor (S) is 118% (at the bias voltage of 0.17 V). This phenomenon explains that the changes in both the dielectric constant and the charge of gas sensitive layer, due to physical absorption and chemical interaction between NO_2 gas and gas sensitive layer, produce $I_{\text{ph}}-V_{\text{bias}}$ shift. The equation of the shift can be defined as follows (with surface potential, $\phi_s = 0$):^{9,10,13}

$$\Delta V_{\text{Bias}} = \frac{Q_{0\text{NO}_2}}{C_{i\text{NO}_2}} - \frac{Q_0}{C_i} = \frac{Q_0 + \Delta Q_0}{\epsilon_i + \Delta \epsilon_i} - \frac{Q_0}{\epsilon_i} d \quad (2)$$

$$\Delta V_{\text{Bias}} = \frac{\epsilon_i \Delta Q_0 - \Delta \epsilon_i Q_0}{(\epsilon_i + \Delta \epsilon_i) \epsilon_i} d$$

Where ΔQ_0 , $C_{i\text{NO}_2}$, and $\Delta \epsilon_i$ correspond to the difference of charge density, capacitance in NO_2 , and the dielectric constant, respectively.

In conclusion, the mesoporous tin oxide thin films has been successfully prepared as 1 ppm NO_2 gas sensor using SPV technique.

References

- 1 S. W. Massey, *Sci. Total Environ.*, **227**, 109 (1999).
- 2 N. Miura, S. Yao, Y. Shimizu, and N. Yamazoe, *Sens. Actuators, B*, **13-14**, 387 (1993).
- 3 N. Yamazoe and N. Miura, *Sens. Actuators, B*, **20**, 95 (1994).
- 4 Ulagappan and C. N. R. Rao, *Chem. Commun.*, **1986**, 1685.
- 5 J. W. Hammond and C. Liu, *Sens. Actuators, B*, **81**, 25 (2001).
- 6 Y. Wang, C. Ma, X. Sun, and H. Li, *Microporous Mesoporous Mater.*, **49**, 171 (2001).
- 7 T. Hyodo, N. Nishida, Y. Shimidzu, and M. Egashira, *Sens. Actuators, B*, **83**, 209 (2002).
- 8 T. K. H. Starke, G. S. V. Coles, and H. Ferkel, *Sens. Actuators, B*, **85**, 239 (2002).
- 9 H. S. Zhou, T. Yamada, K. Asai, I. Honma, H. Uchida, and T. Katsube, *Jpn. J. Appl. Phys., Part 1*, **40**, 7098 (2001).
- 10 T. Yamada, H. S. Zhou, H. Uchida, M. Yomita, Y. Ueno, I. Honma, K. Asai, and T. Katsube, *Microporous Mesoporous Mater.*, **54**, 269 (2002).
- 11 Y. Kanai, M. Shimidzu, H. Uchida, H. Nakahara, C. G. Zhou, and H. Maekawa, *Sens. Actuators, B*, **20**, 175 (1994).
- 12 T. Yamada, H. S. Zhou, H. Uchida, M. Tomita, Y. Ueno, T. Ichino, I. Honma, K. Asai, and T. Katsube, *Adv. Mater.*, **14**, 812 (2002).
- 13 D. K. Schroder, *Meas. Sci. Technol.*, **12**, R16 (2001).
- 14 P. Yang, D. Zhao, D. I. Margolese, B. F. Chmelka, and G. D. Stucky, *Chem. Mater.*, **11**, 2813 (1999).
- 15 S. J. Gregg and K. S. W. Sing, in "Adsorption, Surface Area and Porosity," Academic Press, London (1982), Chap. 3.